Influence of CaO on the thermodynamic and transport properties of cobaltous oxide

Z Halem, Jan Kusinski, Nacer Halem, Gianguido Baldinozzi, Georgette Petot Ervas

Influence of CaO on the thermodynamic and transport properties of cobaltous oxide

Z. Halem[†], J. Kusinski[‡], N. Halem[§], G. Baldinozzi[||], G. Petot Ervas[||]

† University of Bouira, (Algeria)
‡ AGH University of Science and Technology, 30059 Krakow (Poland)
§ Laboratory LEC2M, University Mouloud Mammeri, Tizi Ouzou (Algeria)
|| Université Paris-Saclay, Centralesupélec, CNRS, Laboratoire SPMS, 91190 Gif-sur-Yvette (France)

Abstract

The electrical conductivity of Ca-doped $Co_{1-x}O$ single crystals was measured as a function of oxygen partial pressure, over the temperature range 1273-1673 K. The results were analyzed using Seebeck coefficient measurements, microstructural characterizations, EELS and X-ray diffraction experiments. From this set of results, we have shown that the influence of calcium on the thermodynamic and transport properties of cobaltous oxide is due to the reducing behavior of these cations, leading to both the shift of the Co/CoO phase boundary to higher P_{O2} and the formation of singly ionized cobalt cations (Co^{+}) in the stability range of CoO.

Key words: Electrical conductivity, chemical diffusion, Seebeck coefficient, EELS analyses, X-ray diffraction, ionic and electronic defects, Ca reducing behavior, phase boundary.

1 INTRODUCTION

$Co_{1-x}O$ is a member of an important series of transition metal oxides having a rocksalt structure and displaying p-type semiconduction at high temperature, as NiO for instance [1-11]. The prevailing point defects are α times negatively ionized cationic vacancies and electron holes, whose concentrations are determined by the thermodynamic equilibrium with the surrounding atmosphere, but also by the presence of diluted aliovalent cations. However, although calcium cations are divalent, it is apparent from the results of a previous study, that Ca^{2+} behaves as a reducing cation in NiO [8].

In this work, we report a study of the thermodynamic and transport properties of Ca-doped $Co_{1-x}O$ single crystals, to acquire complementary information on the influence of calcium on the thermodynamic and transport properties of transition metal oxides, in order to better understand its doping effect and its reducing behavior in NiO [8] and observed in FeO [12]. Electrical conductivity results were analyzed from microstructural characterizations, Seebeck coefficient measurements, EELS and X-ray diffraction experiments.

2 EXPERIMENTAL RESULTS

The experimental arrangement is shown in Fig.1a. Electrical conductivity measurements were performed using square coupons (5x2x2 mm) cut from a single crystal, grown in an arc image furnace from high purity Johnson Mattey powders (maximum impurity level lower than 30 ppm). The measurements were performed by the four-probe method, at 1.5 kHz, using a double Kelvin bridge (Fig.1b) where the electrical equilibrium was checked by a lock-in fast detection amplifier (G). A thin layer of platinum was applied to the two opposite lower surfaces of the parallelepipedic sample (5x2x2 mm) connected to the voltage sources (Fig.1b), to ensure an uniform repartition of the current lines through the sample. Platinum wires were used as electrical junctions. The oxygen partial pressure was measured near the sample by a yttria-stabilized zirconia gauge [10,11].

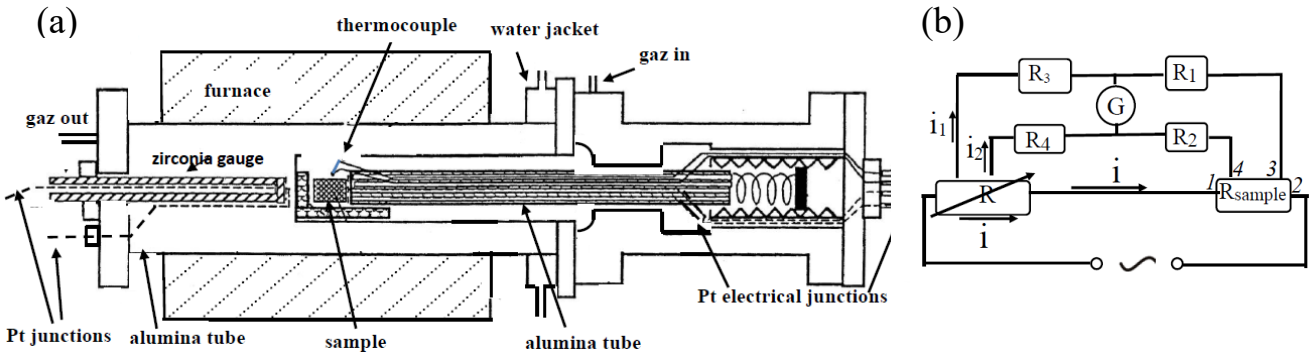

Figure 1- Experimental arrangement for measuring electrical conductivity and schematic representation of the Kelvin bridge.

2.1 Electrical conductivity at the thermodynamical equilibrium.

One can briefly recall that in transition metal oxides, such as CoO or NiO [1-4], the prevailing intrinsic defects are electron holes (h°) and α times negatively ionized cationic vacancies ($V_M^{\alpha'}$), whose concentrations depend upon of both temperature (T) and oxygen partial pressure (P_{O2}) in equilibrium with the sample ($\frac{1}{2}O_2 <=> O_O + V^{\alpha'} + \alpha h^{\circ}$):

$$[h^{\bullet}] = \alpha[V_{Ni}^{\alpha'}] = A(K_V)^{1/(\alpha+1)} (P_{O2})^{1/2(\alpha+1)} \quad (1)$$

where O_O is an oxygen ion on a normal anionic site, $A=\alpha^{1/(\alpha+1)}$, K_V the equilibrium constant of formation of the defects and the square brackets denote molar concentrations.

Consequently, the electrical conductivity (σ) of these oxides is controlled by electron holes ($h^{\bullet}$), due to the higher mobility of these defects ($\mu_h \approx 10^4 \mu_{V\alpha}$) [1,13]:

$$\sigma = e\,\mu\,p = \sigma_o (P_{O2})^{1/2(\alpha+1)} \exp(-\Delta H_\sigma)/RT) \quad (2)$$

where e is the charge of the electron, p the hole concentration per cm^3, μ their mobility regarded as a thermally activated hopping process ($\mu = \mu_o \exp -\Delta H_\mu/RT$), ΔH_σ the enthalpy of conductivity defined by the relation $\Delta H_\sigma = \Delta H_\mu + \Delta H_V/(1+\alpha)$, ΔH_V the enthalpy of formation of the defects, ΔH_μ

the hole enthalpy of mobility, and α the mean charge of the defects that can be determined from the slopes of the experimental diagrams, with [7-11],:

$$(d\ln\sigma / d\ln P_{O2})_T = 1/2(\alpha+1) \qquad (3)$$

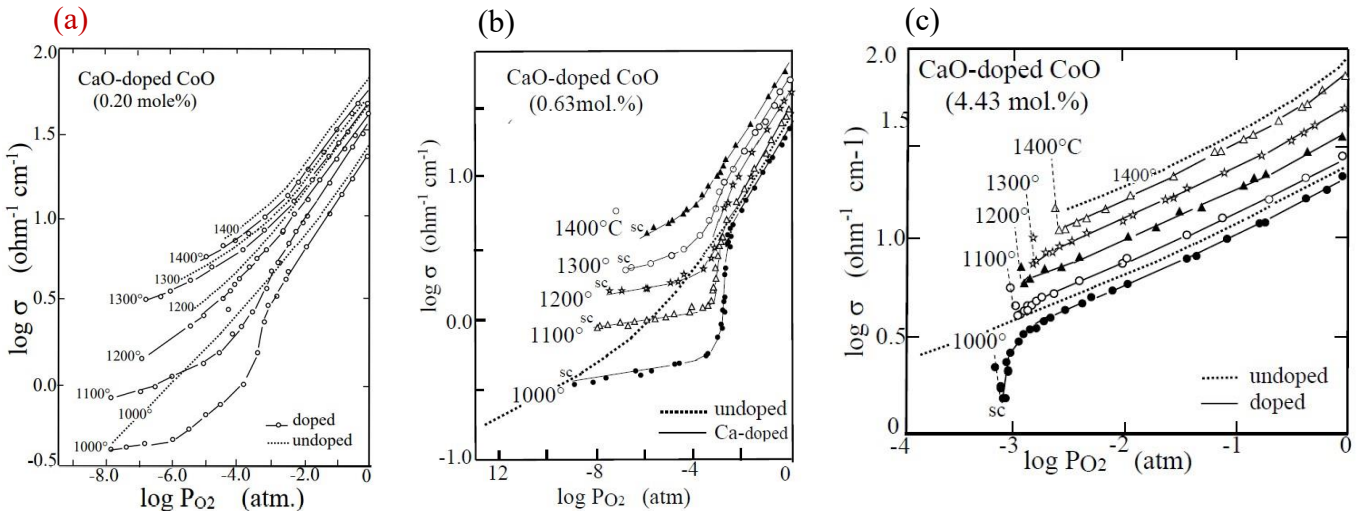

Figure 2 - Electrical conductivity of Ca-doped $Co_{1-x}O$ single crystals. Comparison with the values measured in undoped $Co_{1-x}O$, at 1000°C [7].

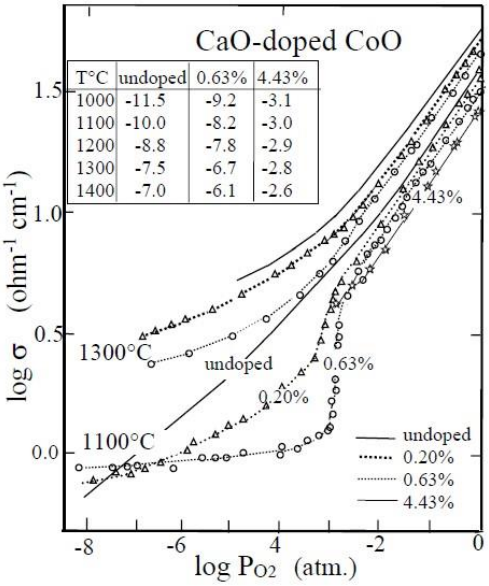

Figure 3 - Influence of the calcium concentration on the electrical conductivity of Ca-doped $Co_{1-x}O$ single crystals, at 1100° and 1300°C.

The dissociation pressure (log P_{O2}) of undoped and Ca-doped (0.63%, 4.43%) CoO is reported (table) between 1000° and 1400°C.

In Figs 2 and 3, we have reported the electrical conductivity values measured for undoped [7] and doped (0.20, 0.63, 4.43 mol% CaO) $Co_{1-x}O$ single crystals, as a function of log P_{O2}. First, these figures show that the values of σ are smaller for the doped samples than those of undoped CoO, and all the more as the calcium content increases. These results suggest then a doping effect of calcium while these cations are apparently divalent as those of cobalt. Indeed, for undoped and doped samples and at $P_{O2}>10^{-3}$atm, the slopes of the curves ($d\ln\sigma / d\ln P_{O2}$) are very closes (Figs.2,3), indicating that the mean charge of the cationic vacancies (Eq.3) is controlled by

reaction with the surrounding atmosphere (Eqs.1,2), as in undoped CoO. While, for $P_{O2}<10^{-3}$atm, these slopes show a greater decrease of σ compared to those of undoped CoO, indicating a calcium doping effect due to a more important decrease of the electron hole concentration in the doped samples. Furthermore, short circuits (denoted ″sc″/Figs.2b,2c) are observed for the two most doped single crystals, indicating the precipitation of a metallic phase which occurs at P_{O2} increasing with the calcium amount (Fig.3/Table). It should be mentioned that these short–circuit occur almost immediately after the decrease of P_{O2}. They are due to the formation of a cobalt film on the surface of the sample, which requires increasing P_{O2} as soon as possible to avoid the deterioration of the single crystal.

One can recall that similar results were found for Ca-doped $Ni_{1-x}O$ single crystals [8,9]. Divalent calcium cations (Ca^{2+}) also act both as a reducing component, leading to the shift of the $Ni/Ni_{1-x}O$ phase boundary to higher P_{O2}, and as a dope influencing the thermodynamic and transport properties of nickel oxide.

2.2 Electrical conductivity in the transient state - Chemical diffusion

The chemical diffusion coefficient was determined for single crystals, initially in thermodynamical equilibrium with the surrounding atmosphere (argon/ $P_{O2}=10^{-3}$atm), by following the electrical conductivity values after a sudden change of P_{O2} (air / $P_{O2}=0.21$atm) [7-12]. A concentration gradient of cationic vacancies (dC_V/dz) sets up immediately near the surfaces of the single crystal, leading to a flux of cationic vacancies coupled to an opposite flux of cations near the surfaces. These fluxes progress in the bulk, pass through a maximum and disappear when the sample has reached its new thermodynamical equilibrium conditions. According to the Fick's law, they may be written in the z direction as [1-3, 11]:

$$J_V=-\Sigma Ji=-\tilde{D}\ (dC_V/dz) \qquad (4a)$$

where $\tilde{D}$ (or D_{chim}) is the chemical diffusion coefficient, that allows to determine both the time to reach the new equilibrium and the mean penetration depth (Δz) of the oxidation (or reduction) front in the oxide, after a time t:

$$(\Delta z=\sqrt{\tilde{D}t}). \qquad (4b)$$

On the other hand, it was demonstrated, from the general equation $(\sigma(t)-\sigma_\infty)$ as a function of time [11], that only the first term of this relation subsists when the time increases:

$$\frac{\sigma(t)-\sigma_\infty}{\sigma_0-\sigma_\infty}=\left(\frac{8}{\pi^2}\right)^3\exp\left[-\pi^2\left(\frac{1}{H^2}+\frac{1}{L^2}+\frac{1}{l^2}\right)\tilde{D}t\right] \qquad (5)$$

where *H*, *L*, *l* are the sample dimensions, σ_0 the initial electrical conductivity when P_{O2} is abruptly changed and σ_∞ the conductivity when the new equilibrium is reached.

Therefore, the chemical diffusion coefficient $\tilde{D}$ can be directly determined from the linear part of the representations [11]:

$$\log \frac{\sigma(t)-\sigma_\infty}{\sigma_0-\sigma_\infty} = f(t) \qquad (6)$$

The Arrhenius plot of the values of $\tilde{D}$ obtained with two Ca-doped $Co_{1-x}O$ single crystals is reported in Fig.4, together with the data determined for undoped $Co_{1-x}O$ [7]. This figure shows that calcium leads to an increase of $\tilde{D}$, in agreement with the results obtained for $Ni_{1-x}O$ [8].

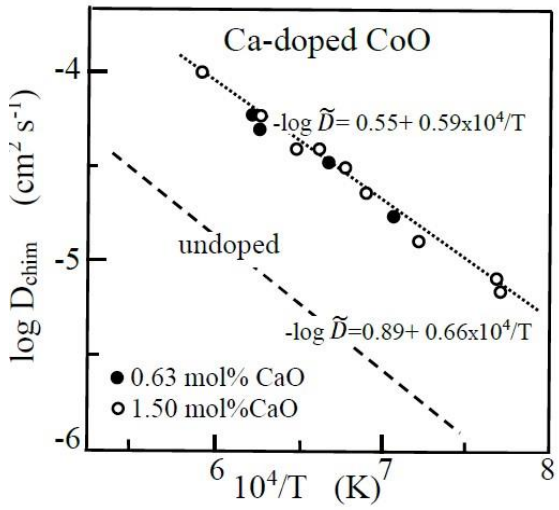

Figure 4- Influence of calcium on the chemical diffusion coefficient of cobalt oxide single crystals. Comparison with the values obtained with undoped $Co_{1-x}O$ [7]

Furthermore, taking into account that the kinetic demixing processes are negligible in these experiments performed with diluted solid solutions, it was shown [10] that the chemical diffusion coefficient of undoped and doped $Ni_{1-x}O$ or $Co_{1-x}O$ single crystals may be expressed by the following relation:

$$\tilde{D} \approx (1+\alpha)D_V \qquad (7)$$

where D_V is the diffusion coefficient of the cationic vacancies ($V_M^{\alpha'}$).

Therefore, according to the similar values of the average charge (α) of the cationic vacancies in the doped and undoped single crystals, for $P_{O2}>10^{-3}$ atm (Eq.3, Figs 2-3), it follows that the greater chemical diffusion values determined for the Ca-doped single crystals (Fig.4) can be explained by an increase of the diffusion coefficient of the cationic vacancies (Eq.7):

$$D_V(\text{Ca-doped CoO}) > D_V(\text{undoped CoO}) \qquad (8)$$

2.3 Seebek coefficient (or thermoelectric power).

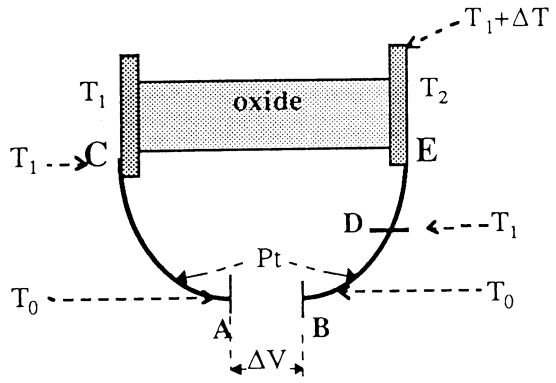

Figure 5- Experimental arrangement for measuring the Seebeck coefficient

In order to better understand the influence of calcium on the electrical conductivity values (Figs.2,3), we have carried-out Seebeck coefficient measurements (Q). Briefly, one can recall that this coefficient is due to the diffusion of the electronic defects toward the cold edge of the sample, whose polarity then gives the sign of the prevailing electronic carriers [14,15]. In strongly p-type semiconducting oxides electron holes (h°) are majority carriers and Qp>0, while in strongly n-type semiconducting oxides, electrons (e') prevails and Qn<0. However, in mixed conducting oxides, the contribution of both charge carriers (h°,e') remains significant. The Seebeck coefficient (Qm) can then be either positive or negative, depending of the relative values of the electronic transference number ($t_{e/h}$) [2,8,14,15]:

$$Q_m = t_h Q_p + t_e Q_n = t_h (k/e) [\ln(A_p/p) + B_p] + t_e (k/e) [\ln(A_n/n) + B_n] \quad (9)$$

where A_n/n and A_p/p denote the concentrations (per cm^3) of the atoms over which the electronic defects hop, B a transport constant, e the charge of the electrons and k the Boltzmann constant.

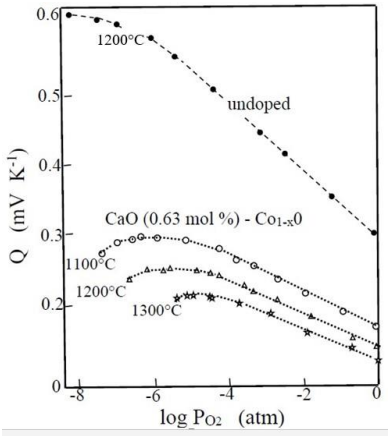

Figure 6 - Seebeck coefficient of undoped [13] and Ca (0.63mol.%)-doped $Co_{1-x}O$ single crystals, as a function of P_{O2}

The Seebeck coefficient determined for undoped [13] and Ca (0.63 mol.% CaO)-doped $Co_{1-x}O$ samples are displayed in Fig.6. These data show that the doped samples are p-type semiconducting oxides (Q>0) in all the P_{O2} range investigated, in agreement with the electrical conductivity results (Figs 2), and the Seebeck coefficient values are lower than those of undoped CoO [13]. However, for $P_{O2}<10^{-4}$ atm, the decline of the positive values of Q ($\frac{dQ}{d\log P_{O_2}} > 0$)

indicates the presence of electrons, leading to a mixed conductivity when the oxygen partial pressure in equilibrium with the sample decreases. It should be noted that this occurs in a range of oxygen partial pressure where a more pronounced decrease of the electrical conductivity is observed in Ca –doped CoO single crystal (Figs.2a,b).

2.4 Microstructural characterizations.

Thin plates were prepared from undoped and Ca-doped CoO single crystals, previously annealed at 1100°C either under air (P_{O2}=0.21atm) or under $P_{O2}=10^{-4}$atm, and rapidly cooled at the end of the thermal treatment. Transmission electron microscopy (TEM) examinations show the presence of Co_3O_4 precipitates in undoped and CaO-doped CoO single crystals annealed under air (Figs.7,8). Their concentrations and sizes increase with the calcium concentration (Fig.7a,8). These precipitates disappear when the samples are annealed under $P_{O2}=10^{-4}$atm. (Fig.7b).

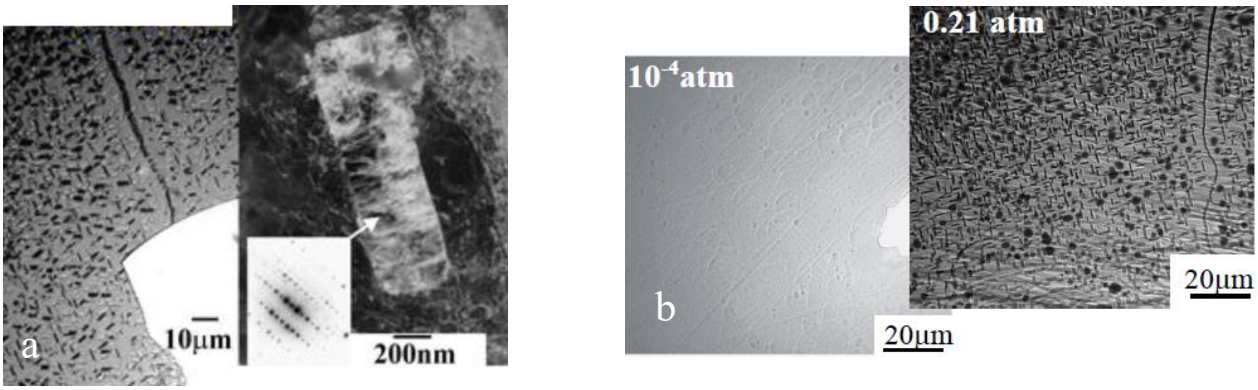

Figure 7- Microstructure of Ca-doped $Co_{1-x}O$ single crystals annealed at 1100°C, for 2h:
(a) Ca(4.43 mol.%)-doped CoO, annealed under air, and bright field image of a precipitate
(b) Ca (0.63mol.%)-doped CoO annealed under 0.21 and 10^{-4} atm

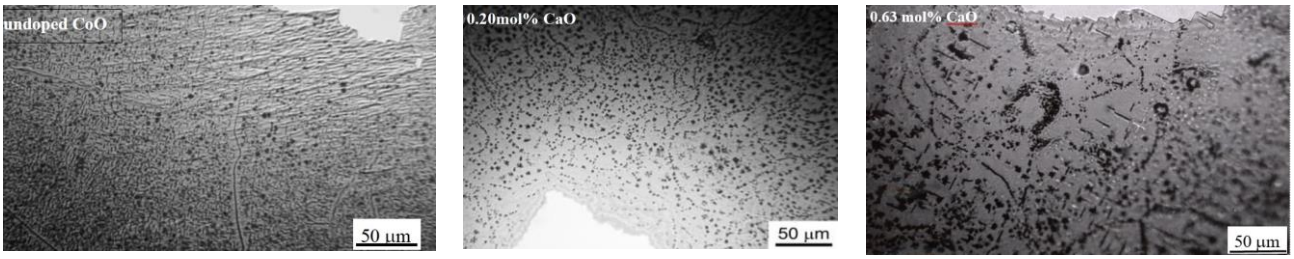

Figure 8 - Influence of the amount of calcium on the microstructure of undoped and Ca (0.20 and 0.63 mol.% CaO)-doped CoO samples annealed under air.

Moreover, energy dispersive spectroscopy (EDS) analysis of a plate prepared from a Ca doped (1.7 mol %)-CoO single crystal, annealed for 2h under air, at 1100°C, did not provide evidence

for calcium in spinel precipitates, the profile intensity across the spinel precipitate being of the same order of magnitude of the measurement errors (Fig.9).

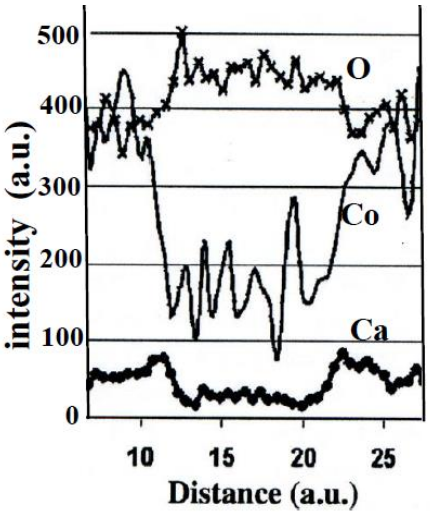

Figure 9 - EDS linear distribution of O, Co and Ca, through the matrix and a Co_3O_4 precipitate.

2.5 X-ray diffraction analyses.

X-rays diffraction analyses were performed in Bragg-Brentano geometry using CuKα radiation and an in-situ Rigaku furnace (RT-1600K) equipped with a controlled gas flow to insure the desired redox condition for the sample. Undoped and doped Ca (4.43 mol% CaO)-doped CoO pristine single crystals were annealed under air, for 2h at 1200°C. When the temperature decreases (Figs.10), they show the appearance of well crystallized Co_3O_4 spinel precipitates that start to appear near 910°C in undoped CoO (in agreement with literature) and at about 1100°C for Ca doped-CoO. Therefore, these results indicate that calcium doping shifts towards higher temperatures the CoO/Co_3O_4 phase boundary, due to an increase of the Co^{3+}/Co^{2+} ratio in the doped samples.

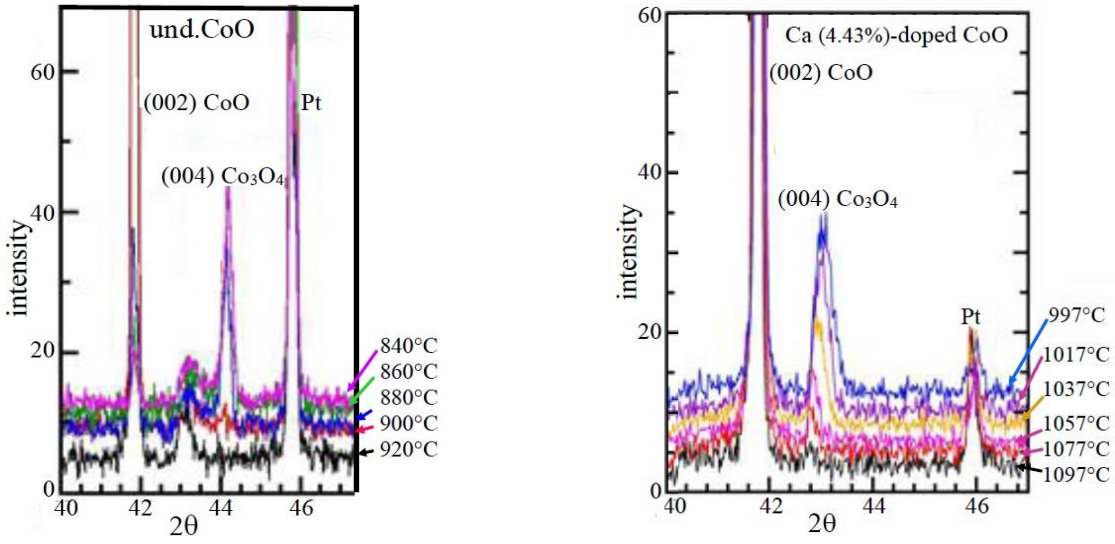

Figure 10–X-ray diffraction analysis as a function of the temperature of undoped and Ca (0.43mol% CaO)-doped CoO single crystals, showing the temperature of Co_3O_4 precipitation, under air flow.

2.6 Electron Energy-Loss Spectroscopy analysis

EELS was used to investigate the effect of calcium over the oxidation state of cobalt and the structure of CoO single crystals [16-18]. The specimens were discs of 3 mm diameter and approximately 0.1mm thickness, cut from single crystals annealed for 2h, either under air or under argon at 1100°C, then cooled at a rate of 300°/min down to 700°C and finally at 70°C/min down to room temperature.

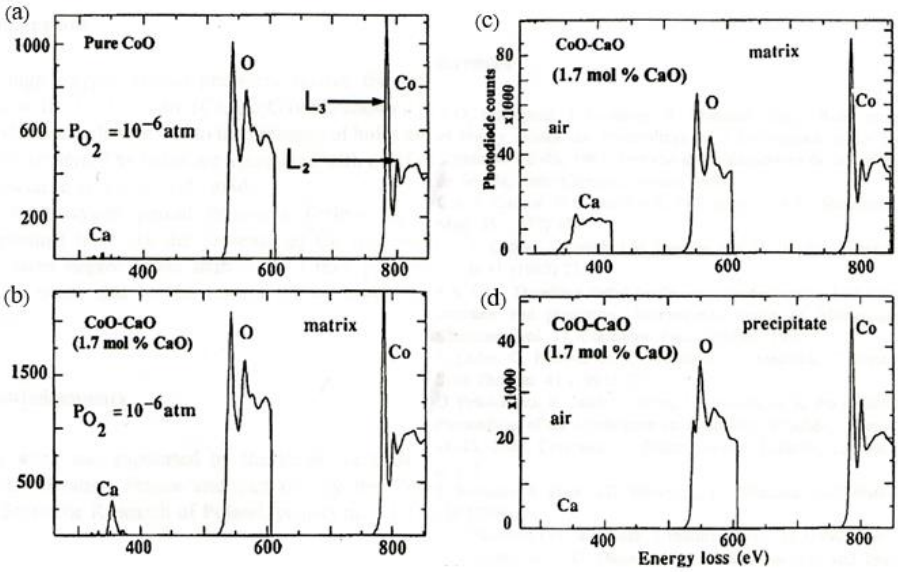

Figure 11- EELS spectra of undoped and Ca (1.7mol.% CaO)-doped CoO single crystals, showing changes of Ca, O K-edges and Co L-edges. EELS spectra of undoped CoO, annealed under air are similar to those of doped CoO, for energy losses higher than 400eV (Fig.11c).

In Figs.11, we have reported EELS spectra of undoped and Ca doped (1.7 mol % CaO) - CoO single crystals [16]. The data for each component appear in three separate regions, showing changes of oxygen, cobalt, and calcium edges.

First, EELS spectra of precipitates show that they do not contain calcium, in agreement with the EDS analysis (Fig.9). These precipitates consist of the pure Co_3O_4 spinel phase (Fig.11d).
Moreover, in Figs 11a,b,c we have reported EELS spectra of the matrix of undoped CoO and (1.7 mol% CaO) Ca-doped CoO single crystals annealed either under air (P_{O2}=0.21 arm) or $P_{O2}=10^{-6}$ atm, respectively [16]. Considering the differences associated with the presence of calcium in the fine structure of the oxygen K edges and cobalt $L_{2,3}$ edges, it is possible to establish:

- that the Co L_3/L_2 intensity ratio of the doped single crystal, annealed under $P_{O2}=10^{-6}$ atm, is slightly higher (R_W=2.39) than in the equivalent sample annealed under air (R_W=2.32) and in undoped CoO annealed under $P_{O2}=10^{-6}$ atm (R_W=2.31),

- a shift of the oxygen K edges and cobalt $L_{2,3}$ edges toward higher energy losses (Figs 11a,b,c), for the samples annealed under air,
- a change of the separation between the cobalt L_3 and cobalt L_2 lines ($\Delta E_{L3/L2}$) for the doped and undoped samples, annealed either under $P_{O2}=10^{-6}$ atm or under air. For doped CoO annealed under 10^{-6} atm (Fig.11b), $\Delta E_{L3/L2}$=19.4 eV, while for the same sample annealed under air, $\Delta E_{L3/L2}$=23.4eV (Fig.11c) (Fig 11c. A similar result is found for undoped CoO).
- For undoped CoO annealed under 10^{-6} atm, $\Delta E_{L3/L2}$=20.1 eV (Fig.11a) is observed, while for the same sample annealed under air, $\Delta E_{L3/L2}$=23.4eV. Moreover, for doped CoO annealed under 10^{-6} atm, $\Delta E_{L3/L2}$=19.4 eV is obtained, while for undoped CoO annealed under the same conditions $\Delta E_{L3/L2}$=20.1 eV is observed.

According to the works of Stemmer et al. [17] and Paterson et al.[18], this set of results indicates first a decrease of the valence state of cobalt in undoped (Fig.11a) and Ca-doped CoO (Fig.11b) samples, when the oxygen partial pressure in equilibrium with the sample decreases. Consequently, due to the presence of cobalt cations twice and three times ionized (Co^{2+}, Co^{3+}) near the CoO/Co_3O_4 phase boundary (Fig. 10), the cations Co^{3+} disappear in the samples when P_{O2} decreases. Furthermore, when these single crystals are annealed under $P_{O2}=10^{-6}$ atm, one has for the doped CoO samples $\Delta E_{L3/L2}$=19.4 eV, while for undoped CoO one has $\Delta E_{L3/L2}$=20.1 eV. These results indicate then a lower valence state of cobalt in Ca-doped CoO than what is observed in undoped CoO counterparts. Therefore, this shows the presence of singly ionized cobalt cations (Co^{+}) in the doped CoO sample when P_{O2} decreases.

3 DISCUSSION

This body of results, obtained by Seebeck coefficient measurements, X-ray diffraction experiments, microstructural examinations, and EELS analysis, allows to explain the unexpected electrical conductivity results, at $P_{O2}<10^{-3}$ atm (Figs.2,3). First, considering the fine structure of oxygen K edges and cobalt $L_{2,3}$ edges of the matrix of undoped and doped CoO single crystals, annealed either under air or under $P_{O2}=10^{-6}$ atm (Fig.11), EELS results show that calcium additions lead to a decrease of the valence state of cobalt when the oxygen partial pressure in equilibrium with the sample decreases. Furthermore, according to in-situ X-ray diffraction results carried out under flowing air, the observed structures confirm the presence of Co^{3+} cations in the Ca-doped samples (Fig.10), which disappear in undoped CoO. Therefore, when these samples are annealed under $P_{O2}=10^{-6}$ atm, the decrease of the valence state of cobalt in the doped sample, in comparison to undoped CoO annealed in the same conditions and undoped CoO annealed under air, indicates the presence of singly ionized cobalt cations (Co^{+}) in the doped single crystals. Consequently, when the divalent cation (Ca^{2+}) is substituted onto a Co^{+} site, the corresponding defect will carry an effective single positive charge ($Ca^{\bullet}_{Co}$) and its formation can be schematically described by the following relation:

$$Ca^{x}_{Co} \Leftrightarrow Ca^{\bullet}_{Co} + e', \qquad (10)$$

This equation explains the presence of electrons and electronic holes observed by Seebeck coefficient measurements from $P_{O2}<10^{-4}$ atm (Fig.6). Therefore, these extrinsic defects ($Ca^{\bullet}_{Co}$, *e'*) influence the concentration of intrinsic defects (Eq.1), through the electroneutrality condition:

$$\alpha[V^{\alpha'}_{Co}]+[e']=[h^{\circ}]+[Ca^{\bullet}_{Co}] \qquad (11)$$

The steeper decrease of the Ca-doped CoO single crystals conductivity (Figs.2) at $P_{O2}<10^{-3}$ atm, occurring near the same oxygen partial pressure where electrons start to be detected from Seebeck coefficient measurements (Fig.6), can then be explained by the reducing behavior of calcium (Eq.10). In other words, these results suggest that the faster decrease of σ is observed when the concentration of the extrinsic defect $Ca^{\bullet}_{Ni}$ is of the same order of magnitude than that of intrinsic defects (Eq.1), leading to a higher decrease of the concentration of electron holes and therefore of σ.

Remark Before concluding, it can be indicated that the reducing behavior of calcium observed in FeO [12] may be due, as in CoO and NiO, to its influence on the thermodynamic properties of this transition metal oxide, leading to the formation of ionized cations once (Fe^{+}) within the stability range of FeO, at low P_{O2}.

4 CONCLUSIONS

X-ray diffraction, Seebeck coefficient measurements and EELS results demonstrate that calcium behaves as a reducing cation in CoO, leading to both, the formation of singly ionized cobalt ions (Co^{+}) within the stability range of Ca-doped CoO and the shift of the Co/CoO and CoO/Co_3O_4 phase boundaries to higher and lower P_{O2}, respectively. The thermodynamical properties of the doped samples within their stability range are then governed by both intrinsic and extrinsic defects. This allows to explain the greater decrease of the electrical conductivity in the doped (0.20 and 0.63 mol% CaO)- CoO single crystals, around $P_{O2}=10^{-3}$ atm. This result is due to the increase concentration of extrinsic defects *(*$Ca^{\bullet}_{Co}$, e'*)* when the oxygen partial pressure (P_{O2}) in equilibrium with the sample decreases (Eqs.1,2). This greater decrease of σ starts to appear when the concentrations of the extrinsic defects $Ca^{\bullet}_{Co}$ is of the same order of magnitude than that intrinsic defects ($V^{\alpha'}_{Co}$, h°) are Furthermore, electrical conductivity measurements in transient state show that the chemical diffusion coefficient is higher in calcium doped samples than in undoped $Co_{1-x}O$, due to an increase of the diffusion coefficient of the cationic vacancies.

Acknowlegements. The authors acknowledge Pr.B..Jouffrey, Centrale Supelec, and Pr.P.Schttscheider,TU Wien, for EELS experiments and discussions of these results, and Pr. C.Petot ,Centrale Supelec, for his interest in this work.

Bibliography

1- P.Kofstad, *Nonstoichiometry, Diffusion and Electrical Conductivity in Binary Metal Oxides*, Wiley Interscience, New York (1972)

2- P.Kofstad, T.Norby, Defects and Transport in Crystalline Solid, (2006)

3- J.Philibert, *Atom movements*, *Diffusion and Mass transport in Solids*, les Editions de Physique les Ullis, France (1991)

4- H.Shmalzried, *Chemical Kinetics of Solids*, Ed. Weinheim N.Y. (1994))

5-K.Hoshino, N.L.Peterson, *Cation impurity diffusion in CoO and NiO*, J.Phys.Chem.Solids, Cation impurity diffusion in CoO and NiO, 45, 963-972 (1984)

6- H.Boussetta, M.Labidi, C.Dolin, C.Monty, *Diffusion du calcium dans $Co_{1-x}O$ monocristallin*, J.Phys. III, 5, 1759-1770 (1995)

7- G.Petot-Ervas, P.Ochin, B. Sossa, *Transport Properties in pure and doped lithium–doped cobaltous oxide*, Solid State Ionic, 12, 277-293 (1985).

8- H.Aïdrous, L.Cieniek, N.Halem, J.Kusinski, C.Petot, G.Petot-Ervas, *Transport properties of Ca-doped nickel oxide and relevance to the oxidation of CaO-coated- Ni,* Sol. St. *Ionics,* 261,117-124 (2014)

9- L.Cieniek, Thesis, AGH- University Science and Technology Krakow and ECP Châtenay Malabry France, 2007

10- Z.Halem, N.Halem, M.Abrudeanu, S.Chekroude, C.Petot, G.Petot-Ervas, *Transport properties of Al and Cr-doped Nickel oxide relevant to the thermal, oxidation of dilute Ni-Al and Ni-Cr Alloys, Solid State Ionics* 297, 13-19 (2016)

11-R.Farhi, G.Petot-Ervas, *Electrical conductivity in single crystalline nickel oxide at high temperature*, J. Phys. and Chem. of Sol., part I, 39, 1169-1173 (1978). *Thermodynamic study of point defects in single crystalline nickel oxide: analysis of experimental results,* J. Phys. and Chem. of Sol., part II, 39, 1175-1179 (1978).

12-C.Monty, G.Petot-Ervas, G.Dhalenne, J.Kusinski, S.Jasienska, Influence of Ca, Mg, Mn, Ce on the reduction and segregation kinetics of FeO. Metalurgia Iodlewnictwo, Kwartalnik, Ed.J.Kazanecki, AGH Wydawnitwo, PWN, Krakow-Varsaw, 17, 469-480 (1991)nitwo

13-G.Petot-Ervas, P.Ochin, T.O.Mason, *Analysis of the mobility of the electronic defects in $Co_{1-\delta}O$*, Transport in non-stoichiometric compounds, Ed.G.Simkowitch, V.Stubican,Plenum Press, N.Y.series B, Physics vol.129, 61-71 (1985)

14- P.Ruello, G.Petot-Ervas, C.Petot, *Electrical conductivity and thermoelectric power of uranium dioxide,* J.Am. Cer. Soc. 88, 604-611 (2005)

15-C.Wagner, *The thermoelectric power of cells with ionic compounds involving ionic and electronic conduction*, Progress in Solid State Chemistry, 7,1-37 (1972)

16-J.Kusinski, G.Petot-Ervas, C.Petot, B.Jouffrey, P.Schattschneider, *Microstructure and nanochemistry of Ca doped cobalt oxide single crystals,* Mat. Chem. and Phys., 81, 308-311(2003).

17-S.Stemmer, A.Sane, N.D. Browning, T.J. Mazanec, *Characterization of oxygen–deficient $SrCoO_{3-\delta}$ by electron energy–loss spectroscopy and Z-contrast imaging*, Solid State Ionics, 130, 71-80 (2000)

18-J.H.Patterson, O.L.Krivanek, ELNES of 3d transition-metal oxides II -*Variation with oxidation state and crystal structure*, Ultramicroscopy, 32, 319-325 (1990)